Limonene magic: noncovalent molecular chirality transfer leading to ambidextrous circularly polarised luminescent π-conjugated polymers†

Yoshifumi Kawagoe, Michiya Fujiki* and Yoko Nakano

Received (in Montpellier, France) 5th December 2009, Accepted 4th January 2010
First published as an Advance Article on the web 12th February 2010
DOI: 10.1039/b9nj00733d

Solvent chirality transfer using (*S*)- and (*R*)-limonenes, which are candidates for renewable volatile bioresources (bp 176 °C/760 Torr or bp 94 °C/68 Torr), allowed for the successful production of optically active poly[(9,9-di-*n*-octylfluorenyl-2,7-diyl)-*alt*-bithiophene] (**F8T2**) particles with circular dichroism (CD) and circularly polarised luminescence (CPL) properties. The particles were rapidly produced by CD-silent **F8T2** with the aid of solvent chirality transfer at 25 °C. The present paper demonstrates the following: (i) through weak intermolecular forces, such as π/π, van der Waals and CH/π interactions, CD-/CPL-active **F8T2** aggregates successfully emerge in a chiral tersolvent system of chloroform (a good solvent), alkanol (a poor solvent) and limonene (a chiral solvent); (ii) the alkanol and the enantiopurity of the limonene greatly affect the magnitude and sign of CD-/CPL-signals; (iii) aggregate size considerably affects the magnitude of the induced CD amplitude; (iv) clockwise and counter-clockwise stirring during preparation do not affect the magnitude of these signals; (v) stirring speed weakly affects the induced CD amplitude and (vi) the order of addition of limonene and methanol to the chloroform solution of **F8T2** greatly affects the magnitude of the induced CD amplitude. To prove the renewability of limonenes, we re-used (*S*)-limonene purified by distilling very impure (*S*)-limonene-containing chloroform, methanol and **F8T2**, which was used and stored in a number of limonene chirality transfer experiments. As expected, the CD-/UV-vis spectra of **F8T2** particles utilizing the renewed (*S*)-limonene gave similar CD-/UV-vis spectra to those using the fresh (*S*)-limonene. Moreover, limonene chirality transfer was possible to obtain two CD-active polymers from CD-silent, poly(9,9-di-*n*-octylfluorenyl-2,7-diyl) (**F8**) and poly[(9,9-di-*n*-octylfluorenyl-2,7-diyl)-*alt*-thiophene] (**F8T1**). The protocol may provide an environmentally friendly, safe and mild process to rapidly produce ambidextrous light-emitting polymers with a minimal loss of starting polymers at ambient temperature, from CD-silent polymers without any specific chiral substituents or chiral catalysts.

Introduction

In 1860, Pasteur alleged that homochirality results from the demarcation line between living matter and non-living matter. Since then, the origin of homochirality has been a popular debate among scientists.[1] Though still the most profound mystery, learning from Nature's elegant bottom-up preference has led to the development of new non-living chiral materials, such as synthetic polymers,[2] supramolecules,[3] liquid crystals,[4] small molecules[5] and organic solid crystals,[6] which have chiroptical signals that enable an investigation of their ambidextrous circular dichroism (CD) and circularly polarised luminescence (CPL) properties.[2–8] Among a number of naturally occurring constituents, enantiomeric pairs of limonenes and terpenes have served as a bridge between the realms of bioresources and artificial materials.

On the other hand, recent understanding of non-classical intermolecular forces has led to new concepts that various intra- and intermolecular weak forces,[9] including van der Waals (∼1.0 kcal mol^{-1}), CH/π (∼0.5 kcal mol^{-1}),[9a] CH/O (∼0.5 kcal mol^{-1})[9b] and CF/Si forces (∼0.001 kcal mol^{-1}),[9d] may play key roles in generating the higher order structures of biopolymers, artificial polymers, supramolecules and molecular crystals. These weak forces offer nearly unlimited opportunities for designing and synthesizing optically active π-conjugated polymers that exhibit elaborated CPL and CD functions from optically inactive (CD-silent) polymers with the aid of a molecular chirality transfer process. With this protocol it is possible to detect invisible noncovalent intermolecular chiral forces existing between chiral molecules and polymers. Actually, in the presence of an intense acid–base interaction (∼10 kcal mol^{-1}), a one-handed helix can be formed from CD-silent poly(4-carboxyphenylacetylene)

Graduate School of Materials Science, Nara Institute of Science and Technology, 8916-5 Takayama, Ikoma, Nara 630-0192, Japan. E-mail: fujikim@ms.naist.jp; Tel: 81-743-72-6040

† Electronic supplementary information (ESI) available: Chemical structures of other CD-silent π-conjugated polymers, ^{1}H NMR of **F8T2**, **F8T1** and **F8** in chloroform-*d* and/or THF-d_8, CD/UV-vis spectra of **F8T2** particles by the normal and reverse addition modes, CD/UV-vis spectra of **F8T2** particles by adding the opposite limonene, CD/UV-vis spectra of **F8T2** particles as a function of membrane filter pore size, CD/UV-vis spectra of **F8T2** as a function of stir speed in CW operation, CD/UV-vis spectra of **F8T2** using the renewed **1*S*** and summary of chiroptical data of **F8T2**, **F8T1** and **F8** by the solvent chirality transfer. See DOI: 10.1039/b9nj00733d

($\sim 10^{-2}$ mol repeating unit per litre), with the helical form induced by a tiny amount of chiral molecular amine ($\sim 10^{-2}$ mol per litre).[10] In the presence of intense hydrogen bonding and its equivalent interactions (5–10 kcal mol^{-1}), one-handed helical supramolecular motifs can be formed sponteneously.[11] However, if amplification of the intermolecular effects in solution is not sufficient due to weak forces, a solvent quantity of chiral molecules is needed.[2d]

The first chiral solvent effect was reported for the emergence of Cotton CD signals due to the chirally twisted form of CD-silent benzyl molecules dissolved in (2*S*,3*S*)-butanediol.[12a] The second example was a helical preference revealed by a study of the CD characteristics of poly(hexylisocyanate) in non-racemic chlorinated chiral solvents.[12b] A further study showed that helix formation can be induced when a poor solvent is employed as a co-solvent in combination with a chiral solvent.[12c] This idea was first proven with the production of CD-active polymer particles from CD-silent polysilane bearing achiral side groups in only a mixture of chiral, non-polar and polar solvents.[2d]

Herein, we demonstrate that when methanol was added at 25 °C to a homogeneous mixture of chloroform and enantiopure (*S*)-(−)-limonene (**1*S***) or (*R*)-(+)-limonene (**1*R***) containing achiral, light-emitting poly[(9,9-di-*n*-octyl-fluorenyl-2,7-diyl)-*alt*-bithiophene] (**F8T2**, Chart 1), optically active **F8T2** particles immediately precipitated. The particles exhibited an intense green coloured CPL ($|g_{CPL}|$ = 0.06–0.07 at 510–517 nm) with an extremely high quantum yield (Φ) of 85–90%, along with intense CD ($|g_{CD}|$ = 0.09–0.11 at 508–513 nm) signals. However, when ethanol was used in place of methanol, the CD signal had the opposite sign, indicating a switch in helicity. Limonene chirality made achiral **F8T2** into ambidextrous circularly polarised functioned polymer particles whose handedness is switchable by the selection of the limonene chirality and of the achiral alcohol. The limonene homochirality transfer also permitted us to obtain the corresponding chiroptical polymers in other CD-silent π-conjugated polymers (Chart 1). Poly(9,9-di-*n*-octyl-fluorenyl-2,7-diyl) (**F8**) resulted in optically active particles that exhibited fairly intense CD and CPL signals: the value of $|g_{CD}|$ decreased to approximately 10^{-4}, two orders of magnitude lower than that of **F8T2** particles. Poly[(9,9-di-*n*-octylfluorenyl-2,7-diyl)-*alt*-thiophene] (**F8T1**) polymer particles provided weaker CD signals than **F8**.

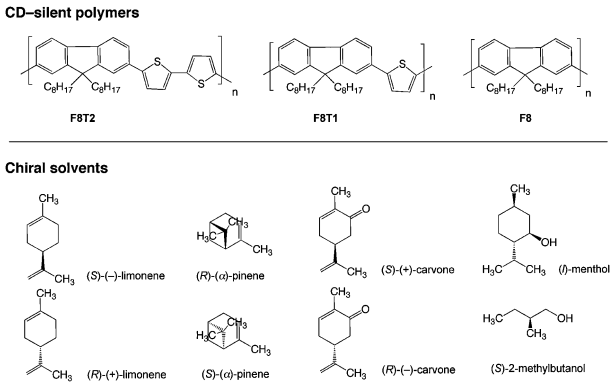

Chart 1 Chemical structures of CD-silent π-conjugated polymers (**F8T2**, **F8T1** and **F8**) and chiral solvents used in this work.

Experimental section

1. Instrumentation

The CD/UV-vis spectra of the solutions were recorded simultaneously at 25 °C on a JASCO J-725 spectropolarimeter equipped with a Peltier-controlled housing unit using an SQ-grade cuvette, with a path length of 10 mm (with a scanning rate of 100 nm min^{-1}, a bandwidth of 1 nm and a response time of 1 s, using a single accumulation). UV-vis spectra were measured independently on a JASCO UV-570 UV-vis–NIR spectrophotometer at 25 °C (with a scanning rate of 100 nm min^{-1}, a bandwidth of 2 nm and a response time of 1 s). Photoluminescence (PL) spectra were measured on a JASCO FP-6500 spectrofluorometer at 25 °C (with a scanning rate of 100 nm min^{-1}, an excitation bandwidth of 3 nm, a monitoring bandwidth of 3 nm and a response time of 1 s). The photoluminescence (PL) quantum yield was determined relative to fluorescein (Φ = 90%, in cyclohexane).[13] The CPL spectrum was recorded on a JASCO CPL-200 spectrofluoropolarimeter, with a path length of 10 mm at room temperature, while the instrument was designed to obtain a high S/N ratio by adjusting the angle between the incident and travelling light to 0° with a notch filter (with a scanning rate of 100 nm min^{-1}, a slit width for excitation of 3000 μm, a slit width for monitoring of 3000 μm and a response time of 1 s). Optical rotation at the Na-d line was measured with a JASCO P-1020 polarimeter with a path length of 1 cm at room temperature. The ^{1}H NMR spectra were recorded with a JEOL EX-400 spectrometer at 400 MHz in $CDCl_3$ at approximately 24 °C. The weight-average molecular weight (M_w), number-average molecular weight (M_n) and polydispersity index (PDI = M_w/M_n) were evaluated using gel permeation chromatography (GPC) on a Shimadzu A10 instrument with PLgel (Varian) 10 μm mixed-B as the column and HPLC-grade THF as the eluent at 40 °C (calibrated with polystyrene standards). The enantiopurity of each limonene was determined using chiral gas chromatography (Spelco, β-DEX-120, 30 mm × 0.25 mm ID, column oven temperature of 85 °C, He as a carrier gas, with a flow rate of 1.2 mL min^{-1}). Fluorescent optical micrographs excited at 450 nm were taken with a Nikon eclipse E400 optical microscope equipped with a Nikon CCD camera. Thermogravimetric (TG) and differential thermogravimetric (DTG) measurements were performed in a stream of N_2 gas (5 °C min^{-1} for heating) using a Seiko Exstar 6200 TG-DTA. The time-resolved PL emission spectra and PL lifetime were measured on a streak camera using a femtosecond laser pulse from an optical parametric amplifier (Hamamatsu Photonics C4780). The centre wavelength of 510 nm was used as the excitation light source (Coherent Mira, Usho KEC-160). Wide-angle X-ray diffraction (WAXD) data was obtained with Rigaku RINT-TTR III/NM (Cu-Kα with Ni filter).

2. Chiroptical analysis[14]

The magnitude of the circular polarisation at the ground state was defined as $g_{CD} = 2\cdot(\varepsilon_L - \varepsilon_R)/(\varepsilon_L + \varepsilon_R)$, where ε_L and ε_R denote the extinction coefficients for left and right circularly

polarised light, respectively. The magnitude of circular polarisation at the excited states is defined as $g_{CPL} = 2\cdot(I_L - I_R)/(I_L + I_R)$, where I_L and I_R denote the output signals for left and right circularly polarised light under unpolarised incident light, respectively. Experimentally, the value of g_{CD} is defined as $\Delta\varepsilon/\varepsilon$ = [ellipticity/32 980]/absorbance at the CD extremum, and for CPL amplitude, the value of g_{CPL} is defined as $\Delta I/I$ = [ellipticity/(32 980/ln10)]/[unpolarised PL intensity] at the CPL extremum.

3. Materials

Spectroscopic grade chloroform, THF, methanol, ethanol and isopropanol (Dotite) were used to prepare the polymer solutions and for measurements. **1*R*** and **1*S*** were obtained from Wako (Tokyo, Japan) and purified by distillation under reduced pressure prior to use. **1*R***: $[\alpha]^{25}_{589} = +100.78^\circ$ (neat), >99.0% *ee*. **1*S***: $[\alpha]^{25}_{589} = -100.97^\circ$ (neat), >99.0% *ee*. Other chiral molecules were purchased from Sigma–Aldrich and used as received. **F8T2** and other π-conjugated polymers were purchased from Aldrich. **F8T2** was purified by precipitation from a chloroform solution of the commercial product with methanol. The ^{1}H NMR spectrum in $CDCl_3$ is given in the ESI, Fig. S1.† **F8T1** was prepared by the Suzuki-coupling reaction of 9,9-dioctyl-fluorene-2,7-diboronic acid (Aldrich) with 2,5-dibromothiophene (Aldrich) and tetrakis(triphenylphosphine)-palladium(0) (Aldrich) according to the published procedure.[15] The ^{1}H NMR spectrum of **F8T1** in THF-d_8 ins given in the ESI, Fig. S2.† The ^{1}H NMR spectrum of **F8** in $CDCl_3$ is given in the ESI, Fig. S3.† Poly(*N*-*n*-decylcarbazoyl-3,6-diyl) was prepared as described in the literature (ESI, Chart S1†) and stored in our laboratory.[16]

4. Preparation of optically active polymer particles

The most typical procedure (called the normal addition mode) used in the present work for the production of **F8T2** aggregates in a mixed **1*R***–chloroform–methanol solvent is described below. First, 2.0 mL of **1*R*** was added to 0.3 mL of a chloroform stock solution containing **F8T2** ($\sim 5 \times 10^{-4}$ M as a repeating unit) in the SQ-cuvette, placed in the Peltier apparatus of a JASCO J725 spectropolarimeter at 25 °C and stirred for 10 s. By addition of 0.7 mL methanol at 25 °C to the solution, a yellowish, turbid solution of **F8T2** particles dispersed in the solvent was instantly formed. After stirring for approximately 10–30 s, this solution was used for the CD/UV-vis and CPL/PL studies. Other π-conjugated polymer particles were obtained in a similar way. The size of **F8T2** particles ranged from 5 to 50 μm, as measured by fluorescent optical microscopy and by evaluating the changes in CD/UV-vis signal intensities with a PTFE membrane filter with different size (1/3/5/10 μm) pores (Millipore).

Results and discussion

Emerging CD/CPL signals from CD-silent F8T2

With the aid of designing chiroptical functional materials by taking advantage of noncovalent, intermolecular, weak chiral forces between non-polar CD-silent polymers and non-polar chiral solvents, we tested ten photoluminescent π-conjugated polymers (Chart 1 and ESI, Chart S1†). These polymers do not contain any chiral centres or specific polar functional groups in their backbones and side chains. We chose eight enantiopure chiral molecules as chiral solvents (Chart 1).

We chose chloroform and THF as achiral good solvents, and we chose methanol, ethanol and isopropanol as achiral poor solvents. To determine whether it is possible to produce an optically active polymer by this approach, we first attempted to optimize the volume fractions in a broad range of mixtures of chiral, good and poor solvents. To quantitatively evaluate the degree of chirality we used the dimensionless chiroptical parameters, Kuhn's dissymmetry factors at the ground and excited states, g_{CD} and g_{CPL}, respectively (Experimental section).[14]

Among the ten polymers tested in this work, optically active **F8T2** particles produced by solvent molecule chirality transfer were of particular significance. The chloroform and total volume of the mixed solvent were fixed at 0.3 mL and 3.0 mL, respectively, and the absolute magnitude of the g_{CD} at the 1st Cotton band of optically active **F8T2** particles varied greatly with the relative volume fraction of **1*R*** and methanol (Fig. 1). This situation was similar to the **1*S*** system. The particle size of **F8T2** was typically 10–100 μm, as measured by fluorescence optical microscopy (Fig. 2).

The most intense CD and CPL spectra of optically active **F8T2** particles produced from CD-silent **F8T2** under the optimized (**1*S*** or **1*R***)–chloroform–methanol mixture [2.0 : 0.3 : 0.7 (v/v/v)] are shown in Fig. 3a and b. A bisignate CD band around 510 and 390 nm clearly emerged in the π–π* transitions of **F8T2**. The sign of an almost mirror-image CD band profile was determined by the limonene chirality, but the value of λ at the extremum (λ_{ext}^{CD}) differs by ~3 nm. The intense CPL signals around 510 and 530 nm appeared in the π–π* transitions of **F8T2**, but the λ_{ext}^{CPL} differs by ~5 nm. The near mirror-image of the CPL band profile depended on the limonene chirality. These CPL bands are derived from the 510 nm CD band. A weak CPL band of the opposite sign near 487 nm can also be distinguished, possibly arising from the 390 nm CD band (Fig. 3b).

The two highest g_{CD} values of **F8T2** were −0.086 (511 nm) and +0.039 (390 nm) from **1*R*** and +0.110 (508 nm) and

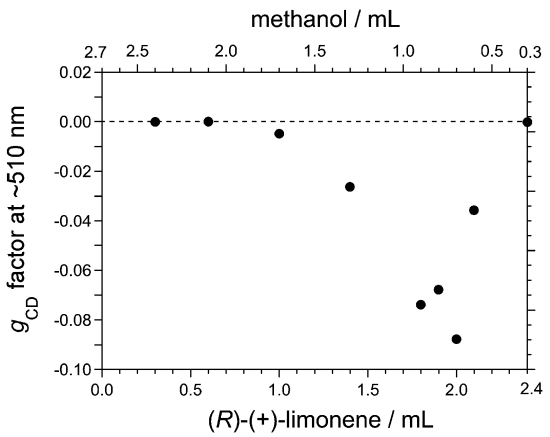

Fig. 1 The g_{CD} values of **F8T2** particles produced in the **1*R***–chloroform–methanol solvent (total 3.0 mL) as a function of methanol and **1*R*** volume fractions.

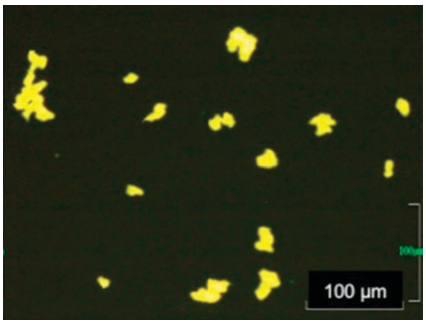

Fig. 2 Fluorescent optical microscopy image (excited at 450 nm) of **F8T2** particles produced in the **1*R***–chloroform–methanol solvent.

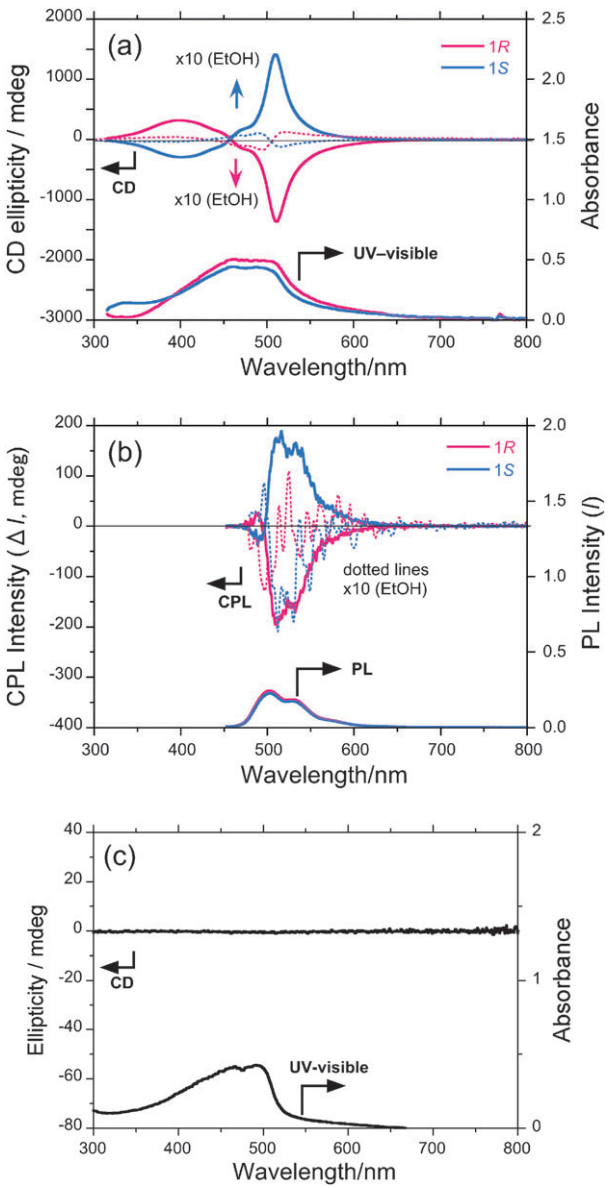

Fig. 3 (a) UV-vis and CD spectra, and (b) PL and CPL spectra of **F8T2** particles (**F8T2**, 1×10^{-5} mol L^{-1}) in limonene–chloroform–alcoholic solvent [2.0 : 0.3 : 0.7 (v/v/v)]; methanol (solid lines) and ethanol (dotted lines), **1*R*** (red line) and **1*S*** (blue line). (c) UV-vis and CD spectra of **F8T2** particles (**F8T2**, 1×10^{-5} mol L) in chloroform–methanol solvent [1.0 : 2.0 (v/v)].

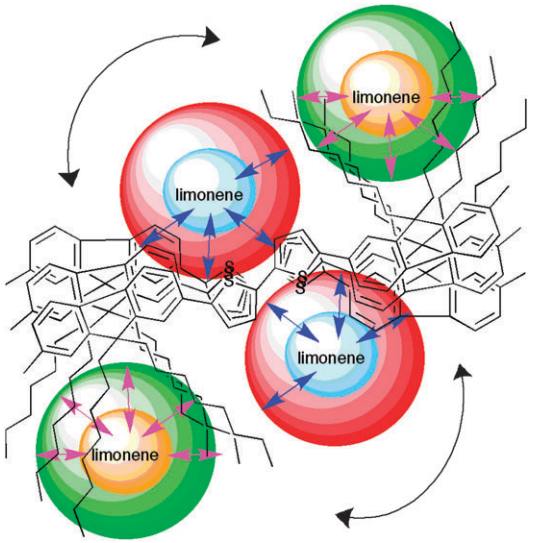

Fig. 4 A proposed model structure of helically ordered **F8T2** π–π stacks with limonene molecules.

−0.040 (395 nm) from **1*S***. Similarly, the two highest g_{CPL} values were −0.063 (~513 nm) and −0.065 (532 nm) from **1*R***, and +0.070 (~517 nm) and +0.066 (533 nm) from **1*S***. These g_{CD} and g_{CPL} values around 510 nm are related to the degree of circular polarisation of 3.3–5.5%, and are almost comparable to the thermally annealed film of poly(*p*-phenylene) bearing achiral pendants that was produced in a chiral nematic liquid crystal host.[17] The signs of the two major 513/517 nm CPL bands are identical to those of the 511/508 nm CD bands and the Stokes shift between the CPL and CD bands is only 2–3 nm. This small shift suggests that **F8T2** particles adopt helically ordered π–π stacks that hold the same chirality at the ground and excited states, as illustrated in Fig. 4.

The Φ values of the particles dispersed in the mixed solvents were 84% for **1*S*** and 91% for **1*R***, which are almost identical to that of 89% for **F8T2** dissolved in chloroform. The similarity in Φ values reflects the fact that there is no significant difference in PL lifetimes between the particles and molecular states: the (*S*)-particles, (*R*)-particles and molecular states had similar PL lifetimes of 0.45 ns, 0.45 ns and 0.50 ns, respectively (Fig. 5).

Limonene homochirality in CD signals of F8T2

The amplification of the most significant helix is known as the majority rule. Optically active chain-like polymers and supramolecular π–π stacks with a preferential screw-sense are nonlinearly amplified by the *ee* value of chiral pendant groups.[2a,11] However, in optically active phthalocyanine (Pc) self-assembling systems, four enantiopure chiral side groups at the peripheral positions (side group homochirality) were inevitably needed to construct helical Pc π–π stacks with one-handed helicity.[18]

Similarly, in the **F8T2**–limonene system, enantiopure limonene was inevitably needed to generate the optically active **F8T2** particles (Fig. 6). A possible reason is that, if **F8T2** forms π–π stacks with **1*S***, the resulting complex acts as a nucleation seed, requiring **1*S*** in the subsequent crystal growth to

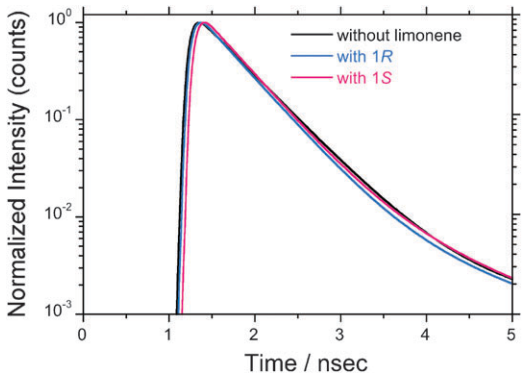

Fig. 5 Photoluminescence dynamics monitored at 510 nm (excited at 450 nm) of **F8T2** that is molecularly dispersed in chloroform (in the absence of limonene) and **F8T2** particle dispersions produced in (**1*R*** or **1*S***)–chloroform–methanol.

maintain one-handed crystal chirality. The antipode limonene disturbs this homochiral crystal growth. Similarly, the opposite handed nuclear seed leads to **F8T2**–**1*R*** crystal growth. We did not observe any detectable CD signals from **F8T2** particles by adding methanol (2.0 mL) to chloroform (1.0 mL) in the absence of **1*S*** and **1*R***. In this case, individual **F8T2** particles may be homochiral but exist as conglomerates (Fig. 3c).

The signs of the weak 485 nm CPL bands from **1*R*** and **1*S*** are identical to those of the corresponding 390 nm CD bands, but the apparent Stokes shift between the CPL and CD bands is as large as ~95 nm. The g_{CPL} values at 390 nm were +0.0094 for **1*R*** and −0.0094 for **1*S***. The 390 nm CD band may originate from magnetically allowed but electronically forbidden π–π* transitions, because an apparent UV-vis band corresponding to the 390 nm CD band cannot be seen. **F8T2** particles produced in a mixture of limonene and methanol did not show any CD and CPL bands in the π–π* transitions. When **F8T2** was homogeneously dissolved in a limonene–chloroform co-solvent, **F8T2** did not show any CD bands in the π–π* transition region, indicating no detectable chiral preference. The weak intermolecular chiral forces between the polymer and these good solvent systems are not efficient. An alcohol, as a poor solvent, is inevitably required to produce optically active **F8T2** particles.

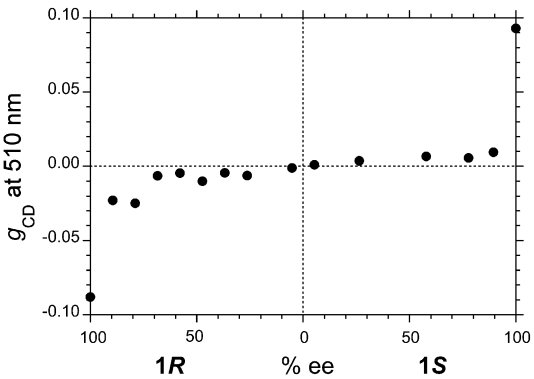

Fig. 6 The g_{CD} value at 510 nm as a function of **F8T2** particles formed in the volume fraction of **1*S*** and **1*R*** in a chloroform–methanol solvent [1.9 : 0.3 : 0.8 (v/v/v)].

Addition order dependency of limonene and methanol

To elucidate the chemical stability of the **F8T2** homochirality, we compared two addition modes of limonene and methanol solvents to the chloroform solution of CD-silent **F8T2** to produce CD-active **F8T2** particles. The normal addition mode refers to the addition of methanol to the homogeneous chloroform–limonene solution containing **F8T2** to produce **F8T2** particles (see Experimental section). The reverse addition mode means the addition of enantiopure limonene to the inhomogeneous chloroform–methanol solution containing **F8T2** particles.

In both cases, the final volume ratio of limonene–chloroform–methanol was kept at 2.0 : 0.3 : 0.7 (v/v/v). The bisignate CD/UV-vis spectral profile of the reverse addition mode showed similar signs and shapes to those prepared by the normal addition mode at the same limonene–chloroform–methanol ratios (ESI, Fig. S4†). However, the g_{CD} values of **F8T2** particles formed by the normal and reverse modes are much different (Fig. 7). The g_{CD} value at the 1st Cotton CD band (~510 nm) of **F8T2** particles prepared by the reverse addition mode with **1*S*** was only approximately one-tenth of that for the normal addition mode. This is very similar to the case of **1*R***. Regardless of the presence of limonene molecules, the production of densely packed π–π stacks as nucleation seeds with the help of methanol might be responsible for the subsequent crystal growth to maintain its crystallinity.

Addition effect of the opposite limonene chirality

As a modification of the reverse addition order mode to verify the homochirality generation hypothesis, we tested two addition modes of **1*S***-to-**1*R***-induced and **1*R***-to-**1*S***-induced **F8T2** particle systems. For the **1*S***-to-**1*R***-induced **F8T2**, 1.0 mL of **1*R*** was added to 0.3 mL of a chloroform solution containing **F8T2** in the cuvette. The addition of 0.7 mL of methanol resulted in the formation of **F8T2** particles. This volume fraction of **1*R***–chloroform–methanol [1.0 : 0.3 : 0.7 (v/v/v)] is not the optimized condition to produce intense CD-active **F8T2** particles (Fig. 3a). The insufficient **1*R*** quantity, leading to loosely stacked π–π aggregates, permits the further addition of the opposite limonene chirality as a solvent. To the solution of **F8T2** particles, 1.0 mL of **1*S*** was added. This protocol was applied to the **1*R***-to-**1*S***-induced **F8T2** particle system. In both

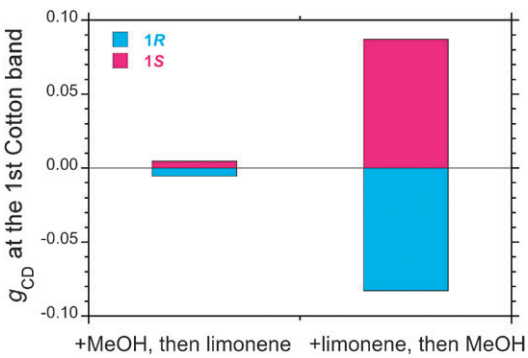

Fig. 7 A comparison between the g_{CD} values of **F8T2** particles formed by the normal and reverse modes in limonene–chloroform–methanol [2.0 : 0.3 : 0.7 (v/v/v)].

cases, the final volume fraction of **1*R***–**1*S***–chloroform–methanol was kept at 1.00 : 1.0 : 0.3 : 0.7 (v/v/v/v) and the limonenes attained a racemic fraction.

Although the bisignate CD/UV-vis spectral profiles of **1*S***-to-**1*R***-induced **F8T2** particles are similar to those prepared by **1*R***-to-**1*S***-induced **F8T2** particle systems (ESI, Fig. S5†), the $|g_{CD}|$ values of **F8T2** particles formed by the **1*R***-to-**1*S*** and **1*S***-to-**1*R*** protocols was greatly diminished, approaching almost CD-silent states (Fig. 8). The greatly diminished induced CD states are comparable to those of the CD-silent **F8T2** particles formed by the normal addition mode of **1*R***–**1*S***–chloroform–methanol (1.0 : 1.0 : 0.3 : 0.7 (v/v/v/v). This is probably due to the slippery nature of the **F8T2** moiety in the π–π stacks in the presence of an insufficient quantity of limonene molecules. In other words, the left- and right-handed preferences of CD-active **F8T2** particles are not stable chemically under insufficient limonene quantity. Hence, it is possible to control the magnitude and sign of the g_{CD} values by the reverse addition order mode using the opposite chirality of limonene molecules in an appropriate volume fraction.

Membrane filter pore-size dependency

The **F8T2** particle size dependency on the CD/UV-vis spectra using membrane filter experiments was examined. The changes in the CD and UV-vis spectra after pressured filtration using a series of different pore sizes are presented in Fig. 9 and in the ESI, Fig. S6.† With pore sizes smaller than 10 μm, the absorbance and CD signals decreased dramatically (ESI, Fig. S6†) and the g_{CD} values depend on the pore size (Fig. 9). Both **1*R*** and **1*S*** produced similar results. By evaluating the half-value in the CD/UV-vis intensities between unfiltered and filtered samples (Fig. 9), the mean aggregate size was estimated as approximately 10 μm. This value is comparable to that of the fluorescent optical microscopy image (Fig. 2). The larger g_{CD} values mainly came from larger crystalline particles. In sharp contrast, an aggregate size dependency was not significant for CD-active polysilane aggregates produced from CD-silent polysilane by a chiral alcohol transfer protocol.[2d]

To elucidate the effect of limonene on CD-active **F8T2** particle growth, WAXD data of **F8T2** particles produced in the limonene–chloroform–methanol mixture and of an unmodified **F8T2** solid were collected. The former has a semicrystalline structure, indicated by the presence of many scattering peaks with a relatively narrow width, while the X-ray pattern of the latter indicated a less crystalline solid, showing a few broad scattering peaks (Fig. 10). The repeating distances of *n*-octyl side chains in **F8T2**–**1*R*** and **F8T2**–**1*S*** were 12.55 and 12.54 Å, respectively, and 12.35 Å in an **F8T2** solid without limonene. The repeating distances between chain backbones of **F8T2**–**1*R*** and **F8T2**–**1*S*** were 4.449 and 4.482 Å, respectively, and 4.308 Å in solid **F8T2** without limonene.[19] The differences in these values are subtle but might be related to the efficient production of CD-/CPL-active **F8T2**.

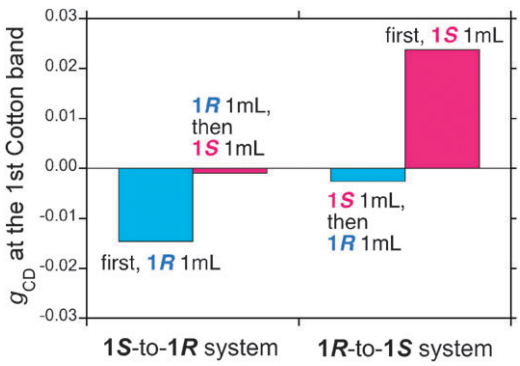

Fig. 8 Addition effects of the opposite limonene to the CD-active **F8T2** particles produced by the normal mode in **1*R***–**1*S***–chloroform–methanol [1.0 : 1.0 : 0.3 : 0.7 (v/v/v/v)].

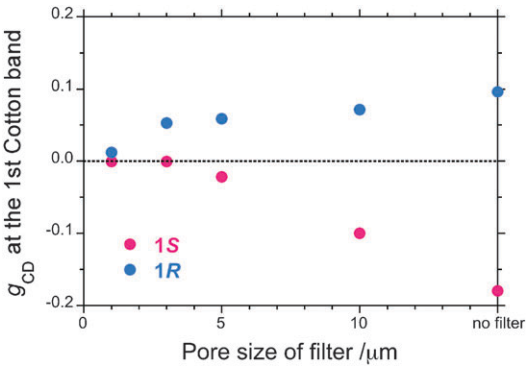

Fig. 9 Changes in the g_{CD} value at the first Cotton CD band of **F8T2** particles produced in limonene–chloroform–methanol [2.0 : 0.3 : 0.7 (v/v/v)], at 25 °C with stirring at 800 rpm (CW), as a function of membrane filter pore size.

Implication of limonene inclusion to CD active F8T2 particles

^{1}H NMR spectra and TG analysis supported the limonene inclusion of 0.10–0.16 limonene molecules per repeat unit of **F8T2** solid, in turn leading to an increase in the crystallinity of **F8T2** with limonene in the **F8T2** particles (Fig. 11 and 12, and ESI, Fig. S1†). The limonene inclusion into the **F8T2** particles could be responsible for the induced CD/CPL properties.

Vortex effect—stirring direction dependency

Recently, a vortex generated by mechanically stirring a fluid solution was reported to induce Cotton CD and linear dichroism (LD) signals that dynamically reflect locally different fluidic

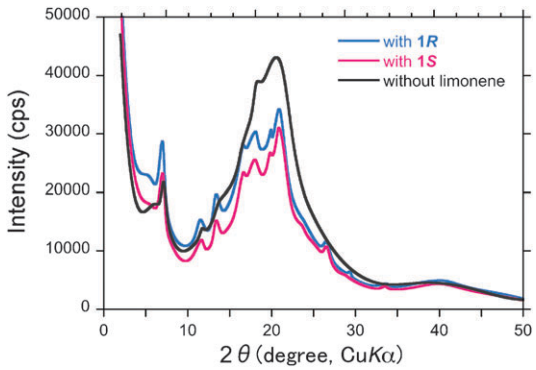

Fig. 10 WAXD data (Cu-Kα with Ni filter) of **F8T2** solids produced with **1*S*** and **1*R*** and an **F8T2** solid without limonene for comparison.

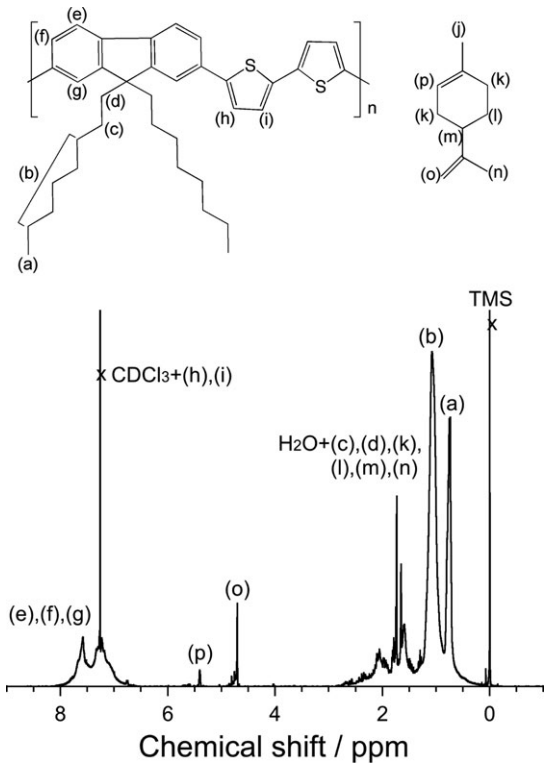

Fig. 11 ^{1}H NMR chart of an **F8T2** solid produced with **1*R*** and re-dissolved in $CDCl_3$. By integrating the ^{1}H NMR signals of protons (o), (p) and (e)–(i), *ca.* 0.1 limonene molecules were included per **F8T2** repeating unit.

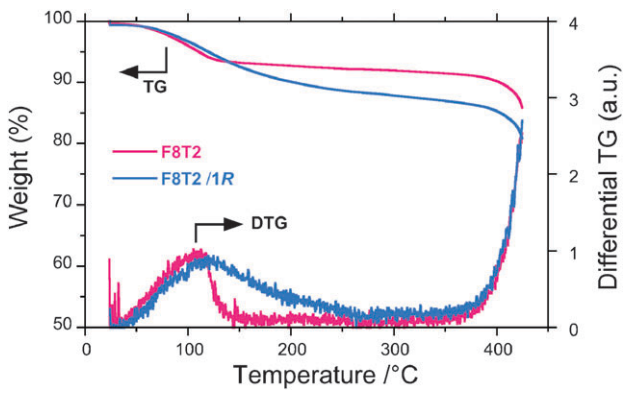

Fig. 12 Thermogravimetric (TG) and differential TG charts of **F8T2** solids produced with and without **1*R***. By calculating the weight loss of **F8T2** with and without **1*R***, a density of 0.16 limonene molecules per **F8T2** repeat unit was calculated.

situations in several molecular systems. A typical example is rod-shaped nanofibers composed of a supramolecularly polymerised zinc porphyrin bearing pyridyl groups and two carboxylic acid groups. These results were due to a temporal alignment of the nanofibers along the chiral fluidic flows.[20] In this study, the LD and CD spectroscopic data of the stirred solutions allowed for a spectroscopic visualisation of the vortex flow.

However, any vortex induction effect[20] was not recognized in the production of the optically active **F8T2** by switching the stirring direction between clockwise (CW, 0–800 rpm) and counter-clockwise (CCW, 0–800 rpm) during the methanol addition (Fig. 13) for five independent runs. The densely packed **F8T2**, with the help of **1*R*** and **1*S***, in semicrystalline solids may be responsible for the efficient limonene homochirality transfer; this principle was demonstrated by the emergence of optically active syndiotactic (st)-polystyrene films when the optically inactive films were dosed with limonene and carvone vapors.[21]

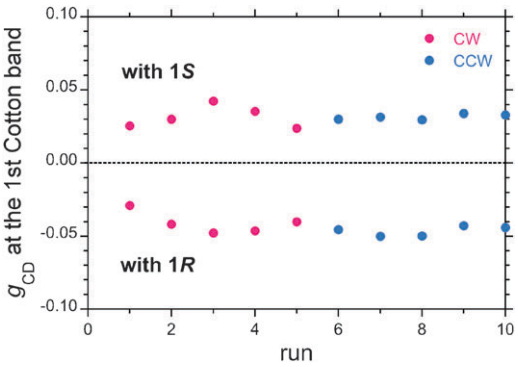

Fig. 13 The g_{CD} value at the 1st Cotton CD band of **F8T2** in chloroform–(**1*S*** or **1*R***)–methanol with five independent CW and CCW runs at 800 rpm.

Vortex effect—stirring speed dependency

Finally, we examined the vortex induction effect,[20] including the stirring direction and stir speed in the cuvette, on the production of the induced CD-active **F8T2** particles. As shown in Fig. 13 and in the ESI, Fig. S7,† any vortex induction effects were not recognized in the production of optically active **F8T2** by switching the stirring direction between clockwise (CW, 800 rpm) and counter-clockwise (CCW, 800 rpm) during methanol addition, for five independent experimental runs. The densely packed **F8T2**, with the help of **1*R*** and **1*S***, in semicrystalline solids might be responsible for the efficient limonene homochirality transfer.

However, weak stir speed dependency of the g_{CD} value of **F8T2** particles was evident when CW stirring and CCW stirring were employed during methanol addition, with stir speeds ranging between 0 and 1000 rpm (Fig. 14). Here 0 rpm means sample mixing by a mild hand-shaking of the cuvette only. The absolute magnitude in the g_{CD} value tends to decrease as stir speed increases from 0 to 1000 rpm. The g_{CD} value at 0 rpm became an almost half-value of that at 1000 rpm regardless of the CW–CCW operation and limonene chirality. Through the addition of methanol under slower stir speeds it may be possible to further increase the absolute g_{CD} value of **F8T2** particles. This work remains as a future issue.

Effects of good solvent, poor solvent and chiral solvents

The proper choice of good solvent, poor solvent and chiral solvent is important to efficiently produce CD-/CPL-active **F8T2** particles. When chloroform was replaced by tetrahydrofuran (THF), the resulting g_{CD} for the limonene–THF–methanol mixture [2.0 : 0.3 : 0.7 (v/v/v)] was of the same sign, but the value of $|g_{CD}|$ decreased by a factor of 4 (ESI, Table S1†). When methanol was replaced by ethanol, the value

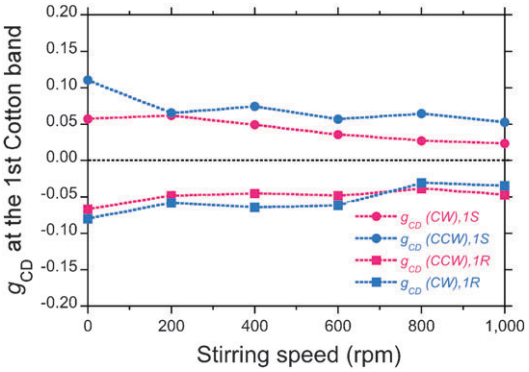

Fig. 14 The g_{CD} value of F8T2 in chloroform–**1*S*** or **1*R***–methanol as a function of stir speed with CW and CCW operations.

of $|g_{CD}|$ in **1*R*** or **1*S***–chloroform–ethanol [2.0 : 0.3 : 0.7 (v/v/v)] was greatly diminished by a factor of 50, but had the opposite sign (Fig. 3a, and ESI, Table S1†), suggesting an inversion of the twisting direction in the π–π stacks, though CPL was nearly non-existent (Fig. 3b). Isopropanol, though very weak in g_{CD} intensity, induces the same sign as the methanol system (ESI, Table S1†).

Additionally, limonene is the most promising chiral solvent among chiral solvent candidates tested in this work (ESI, Table S1†). Limonene gave the highest value ($|g_{CD}| \sim 0.1$). In contrast, (L)-(−)-menthol gave a weaker value ($g_{CD} \sim 0.002$), decreased to ~1/50. Bicyclic (1*R*)-(+)- and (1*S*)-(−)-α-pinenes gave a very weak $|g_{CD}|$ of approximately 0.0005, markedly decreased to ~1/200. Acyclic (*S*)-(−)-2-methylbutanol with monocyclic and (*R*)-(−)- and (*S*)-(+)-carvones did not yield any detectable CD signals.

Limonene chirality transfer experiments on other CD-silent π-conjugated polymers

We explored this limonene homochirality transfer in other CD-silent π-conjugated polymers in an attempt to obtain the corresponding chiroptical polymers (Chart 1, and ESI, Chart S1†). First of all, the effect of the number of thiophene ring spacers between two fluorene rings in a series of fluorene–thiophene alternating copolymers is demonstrated from the viewpoint of PL colour tuning.

F8T1 (M_w = 4.9 × 10^4, PDI = 5.15, Chart 1), which has one thiophene ring as a spacer between two fluorene rings in alternating copolymers, gave a very weak bisignate CD band around 470 and 380 nm (Fig. 15a). PL signals with three well-resolved bands appeared at 466, 497 and 525 nm (Fig. 15b). These wavelength extrema were blue-shifted by approximately 40 nm due to the one-thiophene spacer. However, **F8T1** gave very weak CD signals (Fig. 15a) with $|g_{CD}|$ of 1.3–1.8 × 10^{-4} at 470 nm. The value was lower by three orders of magnitude compared to those in **F8T2** particles. Due to these weaknesses, we did not measure the CPL of **F8T1**.

Emerging Cotton CD/CPL signals from F8

F8 (M_w = 1.2 × 10^4, PDI = 2.93, Chart 1), a derivative of **F8T2** and **F8T1**, gave weak CD signals with a $|g_{CD}|$ value of 3–5 × 10^{-4} at 434 nm, and CPL signals with a $|g_{CPL}|$ value of 3 × 10^{-4} around 433–438 nm. These wavelengths were

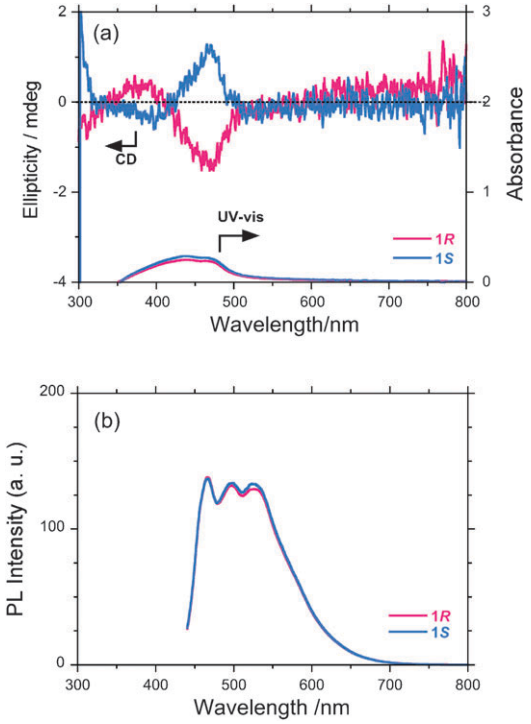

Fig. 15 (a) CD and UV-vis spectra of **F8T1** particles produced in limonene–methanol–chloroform [0.5 : 2.2 : 0.3 (v/v/v)]. **F8T1**: 1.0 × 10^{-5} M per repeating unit. **1*R*** (red line) and **1*R*** (blue line). (b) PL spectra (excited at 432 nm) of **F8T1** particles produced in limonene–methanol–chloroform [0.5 : 2.2 : 0.3 (v/v/v)]. **F8T1**: 1.0 × 10^{-6} M per repeating unit. **1*R*** (red line) and **1*R*** (blue line).

further blue-shifted by approximately 40 nm compared to those of **F8T1** particles due to the lack of thiophene rings. The number of thiophene rings in thiophene–fluorene alternating copolymers is effective at tuning CD- and/or CPL-wavelengths as well as UV-vis and PL wavelengths.[15b] In the **F8T1**–limonene system, the g_{CD} value almost linearly varied with the *ee* value of limonene. Enantiopure limonene was needed to generate the optically active **F8T1** particles (Fig. 16c), because **F8T1** particles are composed of slippery π–π stacks responding to limonene chirality as an external chemical bias.

No emerging CD signals from CD-silent π-conjugated polymers

The other seven CD-silent π-conjugated polymers (ESI, Chart S1†) did not exhibit any detectable CD and CPL signals despite several attempts in several combinatorial approaches using limonene as the best chiral solvent candidate. Subtle differences in main chain and side chain structures of π-conjugated polymers might result from differences in the limonene chirality transfer protocol.

Scope and limitation of limonene chirality transfer

Although the limonene chirality transfer approach is now limited to the generation of CD-/CPL-functionalised **F8T2**, **F8T1** and **F8** particles and cannot apply to all CD-silent π-conjugated polymers, the product yield might be near 100% due to the efficiency of the precipitation method. Among the chiral solvents tested here, **1*S*** and **1*R*** (bp 176 °C, mint/pine

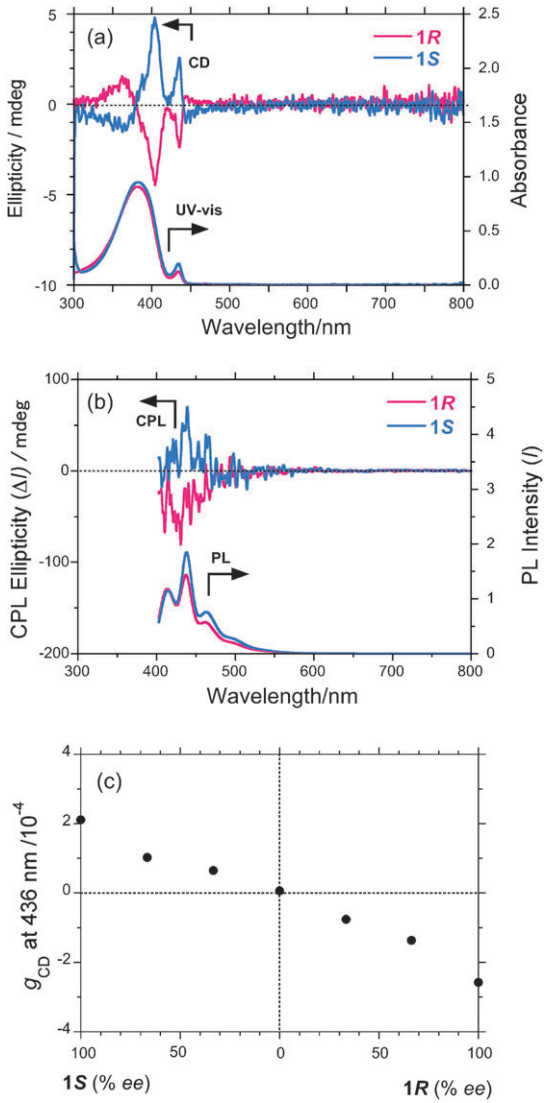

Fig. 16 (a) CD and UV-vis spectra and (b) PL and CPL spectra of **F8** (1.0×10^{-5} M) produced in limonene–chloroform–methanol [1.9 : 0.3 : 0.8 (v/v/v)]. **1*R*** (red line) and **1*S*** (blue line). (c) The g_{CD} value at 430 nm of **F8** particles as a function of enantiopurity of limonene.

and orange/lemon aromas, respectively) are the most promising chiral solvents for producing these ambidextrous chiroptical polymers because they are efficient, inexpensive and renewable bioresources.

To prove the renewability of limonene, we re-used **1*S***, purified by distilling very impure **1*S*** containing chloroform, methanol and **F8T2**, which were used and stored in a number of the limonene chirality transfer experiments. The recovery ratio of **1*S*** was 97% after the distillation under reduced pressure (94 °C at 68 Torr). This is important because **1*S*** (Wako) is twenty times more expensive than **1*R*** (Wako). Actually, the CD-/UV-vis spectra and the g_{CD} value of **F8T2** particles utilizing the recycled **1*S*** (ESI, Fig. S8†) gave similar spectra and properties to **F8T2** using fresh **1*S*** (Fig. 3a).

The CPL-functioned polymer particles may be promising as chiroptical inks for circular polarisation-related applications, such as information storage with security codes. Further elucidation of the transfer mechanism of more efficient solvent chirality transfer protocols suited to most CD-silent π-conjugated polymers is needed in addition to optimisation of the side chain structure of these polymers and a better choice and combination of good, poor and chiral solvents.

Conclusion

The solvent chirality transfer using limonene allows for the successful production of optically active **F8T2** particles with CD-/CPL properties through weak intermolecular forces. Among chiral solvents, **1*S*** and **1*R*** (bp 176 °C, mint/pine and orange/lemon aromas, respectively) may be the most promising chiral solvents for producing ambidextrous chiroptical polymers, because they are efficient, inexpensive and renewable. The chiroptical polymer particles were rapidly produced by CD-/CPL-silent **F8T2** in a controlled chiral tersolvent fraction of chloroform (a good solvent), alkanol (a poor solvent) and limonene (a chiral solvent) at 25 °C. However, the alkanol and enantiopurity of limonene greatly affected the magnitude and sign of the CD-/CPL-signals. Aggregate size considerably affected the magnitude of the induced CD amplitude. Although clockwise and counter-clockwise stirring operations during preparation did not affect the magnitude of these signals, stirring speed weakly affected the induced CD amplitude. Moreover, the order of addition of limonenes and methanol to the chloroform solution of **F8T2** greatly affected the magnitude of the induced CD amplitude. The limonene chirality transfer allowed us to obtain CD- and/or CPL-active polymers from the corresponding CD-silent π-conjugated **F8** and **F8T1**. The protocol demonstrated here will serve a new environmentally friendly, safe and mild process to produce ambidextrous light-emitting polymers, with a minimal loss of starting polymers due to the efficiency of the precipitation method at ambient temperature. Any CD-silent conjugated polymers without any specific chiral substituents and/or chiral catalysts have the possibility to become candidates for CD-/CPL-active polymeric materials in the future. The CPL-functioned polymer particles may be promising as chiroptical inks for circular polarisation-related light emitting device applications.

Acknowledgements

We are grateful for the financial support received from the NAIST Foundation (FY2009), a Grant-in-Aid for Science Research (21655041, FY2009–FY2010) and the Sekisui Chemical Grant Program for Research on Manufacturing Based on Learning from Nature (FY2010). We thank Dr Jun-ichi Kikuchi, Kotohiro Nomura, Masanobu Naito, Wei Zhang and also Satoshi Fukao, Jalilah Binti Abd Jalil, Takashi Mori and Ayako Nakao for fruitful discussions and valuable comments. We thank Yasuo Okajima for measuring PL photodynamics of **F8T2** samples.

References

1 For reviews and books, see: (*a*) G. Wald, *Ann. N. Y. Acad. Sci.*, 1957, **69**, 352–368; (*b*) W. Thiemann and W. Darge, *Origins Life*, 1974, **5**, 263–283; (*c*) S. F. Mason, *Nature*, 1984, **311**, 19–23; (*d*) V. I. Gol'danskii and V. V. Kuz'min, *Sov. Phys. Usp.*, 1989, **32**, 1–28; (*e*) W. A. Bonner, *Origins Life Evol. Biosphere*, 1991, **21**, 59–61; (*f*) L. Orgel, *Nature*, 1992, **358**, 203–209; (*g*) *Advances in Biochemistry*, ed. G. Pályi, C. Zucchi and L. Caglioti, Elsevier, Amsterdam, 1999; (*h*) B. L. Feringa and R. A. van Delden, *Angew. Chem., Int. Ed.*, 1999, **38**, 3418–3438; (*i*) *Chirality in Natural and Applied Science*, ed. L. W. Lough and I. W. Wainer, Blackwell, Oxford, 2002; (*j*) M. Quack, *Angew. Chem., Int. Ed.*, 2002, **41**, 4618–4630; (*k*) K. Soai and T. Kawasaki, *Top. Curr. Chem.*, 2008, **284**, 1–33; (*l*) G. H. Wagniére, *On Chirality and the Universal Asymmetry—Reflections in Image and Mirror Image*, Wiley-VCH, Weinheim, 2007; (*m*) A. Guijarro and M. Yus, *The Origin of Chirality in The Molecules of Life*, RSC Publishing, Cambridge, 2009; (*n*) M. Fujiki, *Chem. Rec.*, 2009, **9**, 271–298.

2 (*a*) M. M. Green, N. C. Peterson, T. Sato, A. Teramoto, R. Cook and S. Lifson, *Science*, 1995, **268**, 1860–1866; (*b*) E. Peeters, M. P. T. Christiaans, R. A. J. Janssen, H. F. M. Schoo, H. P. J. M. Dekkers and E. W. Meijer, *J. Am. Chem. Soc.*, 1997, **119**, 9909–9910; (*c*) M. Fujiki, *J. Am. Chem. Soc.*, 2000, **122**, 3336–3343; (*d*) H. Nakashima, J. R. Koe, K. Torimitsu and M. Fujiki, *J. Am. Chem. Soc.*, 2001, **123**, 4847–4848; (*e*) H. Nakako, R. Nomura and T. Masuda, *Macromolecules*, 2001, **34**, 1496–1502; (*f*) A. P. H. J. Schenning, P. Jonkheijm, E. Peeters and E. W. Meijer, *J. Am. Chem. Soc.*, 2001, **123**, 409–416; (*g*) T. Aoki, T. Kaneko, N. Maruyama, A. Sumi, M. Takahashi, T. Sato and M. Teraguchi, *J. Am. Chem. Soc.*, 2003, **125**, 6346–6347; (*h*) J. Tabei, R. Nomura, F. Sanda and T. Masuda, *Macromolecules*, 2003, **36**, 8603–8608; (*i*) A. Saxena, G. Guo, M. Fujiki, Y. Yang, A. Ohira, K. Okoshi and M. Naito, *Macromolecules*, 2004, **37**, 3081–3083; (*j*) H.-Z. Tang, B. M. Novak, J. He and P. L. Polavarapu, *Angew. Chem., Int. Ed.*, 2005, **44**, 7298–7301; (*k*) G. Lakhwani, S. C. J. Meskers and R. A. J. Janssen, *J. Phys. Chem. B*, 2007, **111**, 5124–5131; (*l*) A. M. Buono, I. Immediata, P. Rizzo and G. Guerra, *J. Am. Chem. Soc.*, 2007, **129**, 10992–10993; (*m*) J. Luijten, E. J. Vorenkamp and A. J. Schouten, *Langmuir*, 2007, **23**, 10772–10778; (*n*) T. Fujii, M. Shiotsuki, Y. Inai, F. Sanda and T. Masuda, *Macromolecules*, 2007, **40**, 7079–7088; (*o*) G. Cipparrone, P. Pagliusi, C. Provenzano and V. P. Shibaev, *Macromolecules*, 2008, **41**, 5992–5996; (*p*) E. Yashima, K. Maeda and Y. Furusho, *Acc. Chem. Res.*, 2008, **41**, 1166–1180; (*q*) E. Yashima, K. Maeda, H. Iida, Y. Furusho and K. Nagai, *Chem. Rev.*, 2009, **109**, 6102–6211; (*r*) K. Akagi, *Chem. Rev.*, 2009, **109**, 5354–5401.

3 (*a*) A. Satrijo, S. C. J. Meskers and T. M. Swager, *J. Am. Chem. Soc.*, 2006, **128**, 9030–9031; (*b*) G. A. Hembury, V. V. Borovkov and Y. Inoue, *Chem. Rev.*, 2008, **108**, 1–73; (*c*) H. Matsukizono, K. Kuroiwa and N. Kimizuka, *J. Am. Chem. Soc.*, 2008, **130**, 5622–5623; (*d*) *Chirality at the Nanoscale: Nanoparticles, Surfaces, Materials and More*, ed. D. B. Amabilino, Wiley-VCH, Weinheim, 2009.

4 (*a*) S. H. Chen, D. Katsis, A. W. Schmid, J. C. Mastrangelo, T. Tsutsui and T. N. Blanton, *Nature*, 1999, **397**, 506–508; (*b*) H. P. Chen, D. Katsis, J. C. Mastrangelo, S. H. Chen, S. D. Jacobs and P. J. Hood, *Adv. Mater.*, 2000, **12**, 1283–1286; (*c*) R. Ozaki, Y. Matsuhisa, M. Ozaki and K. Yoshino, *Appl. Phys. Lett.*, 2004, **84**, 1844–1846; (*d*) S. Furumi and Y. Sakka, *Adv. Mater.*, 2006, **18**, 775–780; (*e*) N. Y. Ha, Y. Ohtsuka, S. M. Jeong, S. Nishimura, G. Suzaki, Y. Takanishi, Y. Ishikawa and H. Takezoe, *Nat. Mater.*, 2008, **7**, 43–47.

5 (*a*) R. A. van Delden, N. P. M. Huck, J. J. Piet, J. M. Warman, S. C. J. Meskers, H. P. J. M. Dekkers and B. L. Feringa, *J. Am. Chem. Soc.*, 2003, **125**, 15659–15665; (*b*) F. C. Spano, S. C. J. Meskers, E. Hennebicq and D. Beljonne, *J. Am. Chem. Soc.*, 2007, **129**, 7044–7054; (*c*) S. Petoud, G. Muller, E. G. Moore, J. Xu, J. Sokolnicki, J. P. Riehl, U. N. Le, S. M. Cohen and K. N. Raymond, *J. Am. Chem. Soc.*, 2007, **129**, 77–83; (*d*) K. Do, F. C. Muller and G. Muller, *J. Phys. Chem. A*, 2008, **112**, 6789–6793; (*e*) J. L. Lunkley, D. Shirotani, K. Yamanari, S. Kaizaki and G. Muller, *J. Am. Chem. Soc.*, 2008, **130**, 13814–13815.

6 (*a*) H. Yao, K. Miki, N. Nishida, A. Sasaki and K. Kimura, *J. Am. Chem. Soc.*, 2005, **127**, 15536–15543; (*b*) Y. Imai, K. Kawano, Y. Nakano, K. Kawaguchi, T. Harada, T. Sato, M. Fujiki, R. Kuroda and Y. Matsubara, *New J. Chem.*, 2008, **32**, 1110–1112; (*c*) Y. Imai, K. Murata, N. Asano, Y. Nakano, K. Kawaguchi, T. Harada, T. Sato, M. Fujiki, R. Kuroda and Y. Matsubara, *Cryst. Growth Des.*, 2008, **8**, 3376–3379; (*d*) S. D. Elliott, M. P. Moloney and Y. K. Gun'ko, *Nano Lett.*, 2008, **8**, 2452–2457.

7 For reviews, see: (*a*) M. Leclerc, *J. Polym. Sci., Part A: Polym. Chem.*, 2001, **39**, 2867–2873; (*b*) A. C. Grinmsdale and K. Müllen, *Adv. Polym. Sci.*, 2006, **199**, 1–82; (*c*) *Polyfluorenes*, *Advances in Polymer Science*, vol. 212, eds. U. Scherf and D. Neher, Springer, Berlin, 2008..

8 (*a*) Q. Pei and Y. Yang, *J. Am. Chem. Soc.*, 1996, **118**, 7416–7417; (*b*) M. Grell, D. D. C. Bradley, M. Inhasekarun and E. P. Woo, *Adv. Mater.*, 1997, **9**, 798–802; (*c*) M. Grell, D. D. C. Bradley, G. Ungar, J. Hill and K. S. Whitehead, *Macromolecules*, 1999, **32**, 5810–5817; (*d*) M. Oda, S. C. J. Meskers, H. G. Nothofer, U. Scherf and D. Neher, *Synth. Met.*, 2000, **111–112**, 575–577; (*e*) M. Oda, H. G. Nothofer, G. Lieser, U. Scherf, S. C. J. Meskers and D. Neher, *Adv. Mater.*, 2000, **12**, 362–365; (*f*) G. Lieser, M. Oda, T. Miteva, A. Meisel, H. G. Nothofer, U. Scherf and D. Neher, *Macromolecules*, 2000, **33**, 4490–4495; (*g*) H.-Z. Tang, M. Fujiki and M. Motonaga, *Polymer*, 2002, **43**, 6213–6220; (*h*) H.-Z. Tang, M. Fujiki and T. Sato, *Macromolecules*, 2002, **35**, 6439–6445; (*i*) A. C. Grimsdale and K. Müllen, *Adv. Polym. Sci.*, 2006, **199**, 1–82; (*j*) Y. Liu, T. Murao, Y. Nakano, M. Naito and M. Fujiki, *Soft Matter*, 2008, **4**, 2396–2401; (*k*) G. Lakhwani and S. C. J. Meskers, *Macromolecules*, 2009, **42**, 4220–4223.

9 For books and reviews, see: (*a*) M. Nishio, M. Hirota and Y. Umezawa, *The CH/π Interaction: Evidence, Nature, and Consequences*, Wiley-VCH, New York, 1998; (*b*) G. R. Desiraju and T. Steiner, *The Weak Hydrogen Bond: In Structural Chemistry and Biology*, Oxford University Press, Oxford, 2001; (*c*) P. Hobza and Z. Havlas, *Chem. Rev.*, 2000, **100**, 4253–4264; (*d*) M. Fujiki and A. Saxena, *J. Polym. Sci., Part A: Polym. Chem.*, 2008, **46**, 4637–4650.

10 (*a*) E. Yashima, T. Matsushima and Y. Okamoto, *J. Am. Chem. Soc.*, 1997, **119**, 6345–6359; (*b*) E. Yashima, K. Maeda and T. Yamanaka, *J. Am. Chem. Soc.*, 2000, **122**, 7813–7814; (*c*) K. Maeda, K. Morino, Y. Okamoto, T. Sato and E. Yashima, *J. Am. Chem. Soc.*, 2004, **126**, 4329–4342; (*d*) K. Maeda and E. Yashima, *Top. Curr. Chem.*, 2006, **265**, 47–88; (*e*) Y. Hase, K. Nagai, H. Iida, K. Maeda, N. Ochi, K. Sawabe, K. Sakajiri, K. Okoshi and E. Yashima, *J. Am. Chem. Soc.*, 2009, **131**, 10719–10732.

11 (*a*) J. J. L. M. Cornelissen, A. E. Rowan, R. J. M. Nolte and N. A. J. M. Sommerdijk, *Chem. Rev.*, 2001, **101**, 4039–4070; (*b*) L. Brunsveld, B. J. B. Folmer, E. W. Meijer and R. P. Sijbesma, *Chem. Rev.*, 2001, **101**, 4071–4098; (*c*) J. van Gestel, A. R. A. Palmans, B. Titulaer, J. A. J. M. Vekemans and E. W. Meijer, *J. Am. Chem. Soc.*, 2005, **127**, 5490–5494.

12 (*a*) B. Bosnich, *J. Am. Chem. Soc.*, 1967, **89**, 6143–6148; (*b*) M. M. Green, C. Khatri and N. C. Peterson, *J. Am. Chem. Soc.*, 1993, **115**, 4941–4942; (*c*) C. A. Khatri, Y. Pavlova, M. M. Green and H. Morawetz, *J. Am. Chem. Soc.*, 1997, **119**, 6991–6995.

13 D. F. Eaton, *Pure Appl. Chem.*, 1988, **60**, 1107–1114.

14 H. P. J. M. Dekkers, in *Circular Dichroism: Principles and Applications*, ed. N. Berova, K. Nakanishi and R. W. Woody, Wiley-VCH, New York, 2nd edn, 2000, ch. 7.

15 (*a*) A. Donat-Bouillud, I. Lévesque, Y. Tao, M. D'Iorio, S. Beaupré, P. Blondin, M. Ranger, J. Bouchard and M. Leclerc, *Chem. Mater.*, 2000, **12**, 1931–1936; (*b*) M. Ranger and M. Leclerc, *Can. J. Chem.*, 1998, **76**, 1571–1577.

16 Z.-B. Zhang, M. Fujiki, H.-Z. Tang, M. Motonaga and K. Torimitsu, *Macromolecules*, 2002, **35**, 1988–1990.

17 H. Iida, A. Nakamura, Y. Inoue and K. Akagi, *Synth. Met.*, 2003, **135–136**, 91–92.

18 R. Rai, A. Saxena, A. Ohira and M. Fujiki, *Langmuir*, 2005, **21**, 3957–3962.

19 O. Werzer, K. Matoy, D.-M. Smilgies, M. M. Rothmann, P. Strohriegl and R. Resel, *J. Appl. Polym. Sci.*, 2008, **107**, 1817–1821.

20 (*a*) J. M. Ribó, J. Crusats, F. Sagués, J. Claret and R. Rubires, *Science*, 2001, **292**, 2063–2066; (*b*) A. Tsuda, M. A. Alam, T. Harada, T. Yamaguchi, N. Ishii and T. Aida, *Angew. Chem., Int. Ed.*, 2007, **46**, 8198–8202; (*c*) M. Wolffs, S. J. George, Z. Tomovic, S. C. J. Meskers, A. P. H. J. Schenning and E. W. Meijer, *Angew. Chem., Int. Ed.*, 2007, **46**, 8203–8205.

21 (*a*) M. Knaapila, V. M. Garamus, F. B. Dias, L. Almásy, F. Galbrecht, A. Charas, J. Morgado, H. D. Burrows, U. Scherf and A. P. Monkman, *Macromolecules*, 2006, **39**, 6505–6512; (*b*) M. Knaapila, F. B. Dias, V. M. Garamus, L. Almásy, M. Torkkeli, K. Leppänen, F. Galbrecht, E. Preis, H. D. Burrows, U. Scherf and A. P. Monkman, *Macromolecules*, 2007, **40**, 9398–9405.